

## Channel separation in the high-order harmonic generation by an atom in intense infrared field and attosecond pulse

© T.S. Sarantseva<sup>1,2</sup>, A.A. Romanov<sup>1,3</sup>, A.A. Silaev<sup>1,3</sup>, N.V. Vvedenskii<sup>1,3</sup>, M.V. Frolov<sup>1,2</sup>

<sup>1</sup>Lobachevsky State University,  
603950 Nizhny Novgorod, Russia

<sup>2</sup>Voronezh State University,  
394018 Voronezh, Russia

<sup>3</sup>A.V. Gaponov-Grekhov Institute of Applied Physics RAS,  
603950 Nizhny Novgorod, Russia

e-mail: sartan86@gmail.com

Received December 11, 2023

Revised January 09, 2024

Accepted January 16, 2024

This work is devoted to the study of the high-order harmonic generation (HHG) induced by two component field with mutually orthogonal polarization of low-frequency and high-frequency components. A new method for separation of HHG channels induced by low-frequency and high-frequency fields based on polarization measurements is proposed. The influence of the initial state symmetry on the efficiency of channel separation is discussed.

**Keywords:** high-order harmonic generation, two-component laser field, ultrashort laser pulses, attosecond pulses, XUV-initiated processes, polarization filtering.

DOI: 10.61011/EOS.2024.01.58292.17-24

High-order harmonic generation (HHG) by atomic systems in strong infrared (IR) low-frequency laser fields is one of the key phenomena in attosecond physics. The feature of this process is a plateau-like structure that occurs in the high-order harmonic spectrum. The cutoff energy of this structure extends to the ultraviolet range [1–3], which allows using the HHG process for producing ultrashort attosecond pulses [4–6]. High-energy HHG photon generating mechanism may be explained within a three-step rescattering model according to which the three HHG steps include the tunnelling ionization, electron propagation along a closed trajectory and recombination into the initial state with emission of a high-energy photon [7]. In the past decade, considerable interest has been attracted to the study of the influence of ultrashort pulses with extreme ultraviolet (XUV) carrier frequency on the HHG process and other photoprocesses in a strong laser field [8–11]. The XUV photon energy is sufficient for the direct ionization of an atomic target resulting in a new HHG channel for which the tunneling mechanism of electron detachment from the parent ion at the first HHG stage is replaced by the XUV-induced ionization. This HHG channel has some advantages over the IR-induced channel. In particular, time delay variation between IR and XUV pulses defines the electron ionization time and further electron trajectory, enabling the properties of emitted harmonics to be controlled [12,13].

Separation of signals from the IR-induced and XUV-induced HHG channels is an important problem in the investigation of HHG in a two-component field that includes

IR and XUV pulses. For collinear geometry, this problem may be solved by reducing the IR field intensity. The probability of tunneling ionization drops exponentially with intensity decrease, resulting in suppression of the HHG process in the IR-induced channel. Decreasing IR field intensity results in reduction of plateau-like structure extension in the IR-induced and XUV-induced channels. Reduction of the plateau cutoff energy may be partially compensated by an increase in the IR field wavelength, which also results in a decrease in harmonic yield in both channels [14,15]. Therefore, it is important to find alternative approaches to the separation of contributions of the IR-induced and XUV-induced channels in the full HHG yield. A recent study [16] proposed a channel separation method based on using the two-component field with mutually orthogonal component polarization. It is shown that in the case of orthogonal geometry, harmonics in the IR-induced and XUV-induced channels are polarized in mutually perpendicular directions, which enables the XUV-induced HHG contribution to be separated by means of fixed-polarization harmonic yield measurement. This work is devoted to the investigation of the influence of the symmetry of the initial atomic target state on the efficiency of the channel separation method proposed in [16]. Atomic units are used throughout this article if not specified otherwise.

Let us consider the interaction between an unpolarized atom with ionization potential  $I_p = \kappa^2/2$  and a two-component field containing a low-frequency IR component and high-frequency XUV component that are linearly

polarized in mutually perpendicular directions,

$$\begin{aligned} \mathbf{F}(t) = & \mathbf{e}_x F_{\text{IR}} f_{\text{IR}}(t) \cos(\omega_{\text{IR}} t) \\ & + \mathbf{e}_y F_{\text{XUV}} f_{\text{XUV}}(t - \tau) \cos(\omega_{\text{XUV}}(t - \tau)), \end{aligned} \quad (1)$$

where  $F_{\text{IR/XUV}}$ ,  $\omega_{\text{IR/XUV}}$ , and  $f_{\text{IR/XUV}}(t)$  are strength, carrier frequency, and envelope of IR or XUV pulses, respectively.  $\tau$  defines the time delay between the IR and XUV pulses. Parameters have been chosen such as the Keldysh parameter for the IR pulse is less than unity,  $\gamma_{\text{IR}} = \omega_{\text{IR}} \kappa / F_{\text{IR}} < 1$ , and interaction with the IR component is described quasi-classically; for the XUV pulse  $\gamma_{\text{XUV}} = \omega_{\text{XUV}} \kappa / F_{\text{XUV}} > 1$ , and its influence may be described in terms of the perturbation theory.

In the absence of laser fields, an atomic system has not the dipole moment. However, the interaction of the laser field (1) with an atomic system induces the time-dependent dipole moment whose Fourier transform  $\mathbf{d}(\Omega)$  fully defines the amplitude for harmonic with frequency  $\Omega$  and polarization vector  $\mathbf{e}_h$ , is induced in the system:

$$\mathcal{A}(\Omega) = \mathbf{e}_h^* \cdot \mathbf{d}(\Omega). \quad (2)$$

In a wide frequency range  $\Omega$  corresponding to the main high-energy plateau, the IR-induced and XUV-induced channels give the main contribution to the full HHG yield. Therefore, the full induced dipole moment is determined by the sum of two terms:

$$\mathbf{d}(\Omega) = \mathbf{D}_0 + \mathbf{D}_1, \quad (3)$$

where  $\mathbf{D}_0$  describes the IR-induced process corresponding to the zero-order perturbation theory in the electric field strength of the XUV pulse, and  $\mathbf{D}_1$  describes the XUV-induced process with the absorption of a single XUV photon at the ionization stage. For symmetry reasons, the vectors  $\mathbf{D}_0$  and  $\mathbf{D}_1$  may be composed from vectors that are in the problem, i.e. IR and XUV pulse polarization vectors,  $\mathbf{e}_{\text{IR}} = \mathbf{e}_x$  and  $\mathbf{e}_{\text{XUV}} = \mathbf{e}_y$ . In the zero-order perturbation theory in the XUV pulse strength, the induced dipole moment expression may contain an unlimited number of vectors  $\mathbf{e}_{\text{IR}}$ :

$$\mathbf{D}_0 = a_0 \mathbf{e}_{\text{IR}}, \quad (4)$$

where  $a_0$  is some  $t$ -even scalar. Harmonic polarization in the IR-induced channel coincides with the IR field polarization. In the first-order perturbation theory in the XUV pulse strength, the field-induced dipole moment should additionally contain one XUV field polarization vector, and the total expression for vector  $\mathbf{D}_1$  may be written as

$$\mathbf{D}_1 = a_1 \mathbf{e}_{\text{XUV}} + b_1 (\mathbf{e}_{\text{IR}} \cdot \mathbf{e}_{\text{XUV}}) \mathbf{e}_{\text{IR}}, \quad (5)$$

where  $a_1$  and  $b_1$  are also  $t$ -even scalars. However, for the field written as (1), the scalar product  $(\mathbf{e}_{\text{IR}} \cdot \mathbf{e}_{\text{XUV}})$  vanishes, and the vector  $\mathbf{D}_1$  appears to be proportional to the XUV field polarization vector. Thus, harmonics in the XUV-induced channel appear to be polarized at the right angle to

the harmonic polarization vector in the IR-induced channel, and this may be used to separate the contributions of the IR-induced and XUV-induced channels. It should be noted that the general symmetry considerations are true for any unpolarized atom independently of the orbital momentum of the valence electron.

The channel separation method based on fixed-polarization harmonic yield measurement was first proposed in [16] for atomic systems with an outer  $p$ -electron. In this study, we calculate the HHG spectra for two simulated atomic systems having outer shells  $s$  and  $p$ . The neon atom with ionization potential  $I_p = 22.3$  eV was chosen as an atomic system with valence  $p$ -electron. The atomic potential shape was calculated by solving the system of the stationary Kohn-Sham equations [17]. Simulation of an atomic system with valence  $s$ -electron used the Coulomb potential  $U(r) = -Z/r$  with effective charge number  $Z = 1.28$  to ensure the coincidence of the ionization potential of the simulated atomic system with the neon ionization potential. Based on solving the time-dependent Schrödinger equation, the interaction between the given atomic systems and the two-component pulse was investigated. The IR component has the intensity  $I_{\text{IR}} = c F_{\text{IR}}^2 / (8\pi) = 4 \cdot 10^{14}$  W/cm<sup>2</sup>, carrier frequency  $\omega_{\text{IR}} = 1$  eV, and envelope

$$f_{\text{IR}}(t) = \begin{cases} \sin^2(\pi t / \mathcal{T}_{\text{IR}}), & t \in [0, \mathcal{T}_{\text{IR}}], \\ 0, & t \notin [0, \mathcal{T}_{\text{IR}}], \end{cases} \quad (6)$$

where  $\mathcal{T}_{\text{IR}} = 20$  fs. The extreme ultraviolet component of the attosecond pulse has the intensity  $I_{\text{XUV}} = c F_{\text{XUV}}^2 / (8\pi) = 4 \cdot 10^{13}$  W/cm<sup>2</sup>, carrier frequency  $\omega_{\text{XUV}} = 30$  eV, and envelope written as

$$f_{\text{XUV}}(t) = \exp(-2 \ln(2) t^2 / \mathcal{T}_{\text{XUV}}^2), \quad (7)$$

where  $\mathcal{T}_{\text{XUV}} = 0.55$  fs. Time delay between the IR and XUV pulses is equal to  $\tau = 8.3$  fs. The fixed-polarization high-order harmonic yield vs. the photon energy is shown in Figure 1: panels (a) and (b) show the results for harmonics polarized along the IR/XUV pulse polarization vector. It can be seen that the plateau cutoff position and oscillation shape differ for harmonics polarized along  $OX$  and  $OY$  axes, respectively. Numerical calculations also show that the yield of harmonics polarized along the IR field polarization direction weakly depends on the XUV pulse parameters, while the yield of harmonics polarized at the orthogonal angle is proportional to the intensity  $I_{\text{XUV}}$ . This suggests that harmonics with the polarization vector  $\mathbf{e}_h = \mathbf{e}_x$  correspond to the IR-induced channel, while the harmonics with the polarization vector  $\mathbf{e}_h = \mathbf{e}_y$  correspond to the XUV-induced HHG channel. Figure 1 shows that the initial state symmetry has small effect on the harmonic yield in the IR-induced channel but appears critical for the HHG process in the XUV-induced channel. For the system with the valence  $s$ -electron, HHG in the XUV-induced channel is suppressed by several orders compared with the initial  $p$ -state case.

The effect of the initial state symmetry on the HHG process in the XUV-induced channel observed in the

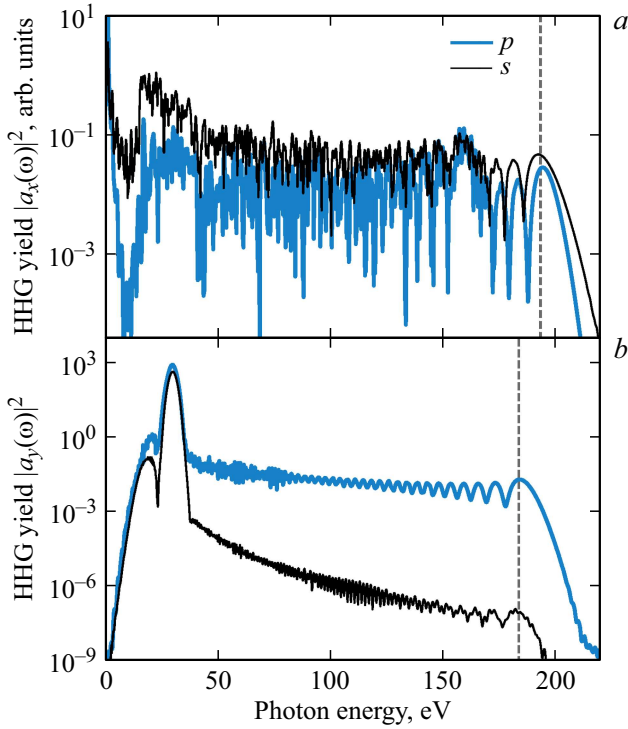


**Figure 1.** The yield of high-order harmonics polarized along the IR field polarization vector (a) and XUV pulse polarization vector (b) vs. photon energy. Thick blue line: the result for Ne atom with the valence  $p$ -electron; thin black line: the result for the simulated system with the valence  $s$ -electron. Vertical dashed lines denote the plateau cutoff position. The two-component pulse parameters are listed in the text.

numerical calculations can be explained in terms of the adiabatic approach to the description of processes in a strong low-frequency laser field [18]. The abovementioned approach is used to derive an expression for amplitudes of processes in strong IR fields in a closed analytical form and to develop the perturbation theory to address the effect of the high-frequency XUV pulse. In terms of the adiabatic approach, the harmonic generation amplitude is fully determined by time moments  $t'_j$  and  $t_j$ , which may be interpreted as the start and end times of electron movement in the strong IR field at the propagation stage. To find these times, the energy conservation law at the time of ionization and recombination is written as

$$\mathbf{K}^2(t'_j; t_j, t'_j) = 2(\omega_{\text{XUV}} - I_p), \quad (8a)$$

$$\mathbf{K}^2(t_j; t_j, t'_j) = 2(\Omega - I_p), \quad (8b)$$

where  $\mathbf{K}(t; t_j, t'_j)$  is an instantaneous value (at  $t$ ) of the electron momentum in motion along the closed trajectory:

$$\mathbf{K}(\tau'; t, t') = \mathbf{e}_x K(\tau'; t, t'), \quad (9a)$$

$$K(\tau'; t, t') = A_{\text{IR}}(\tau') - \frac{1}{t - t'} \int_{t'}^t A_{\text{IR}}(\tau'') d\tau'', \quad (9b)$$

$$A_{\text{IR}}(t) = - \int^t F_{\text{IR}}(\tau') d\tau'. \quad (9c)$$

The dipole moment induced by the two-component field that defines the HHG amplitude in the XUV-induced channel may be written as follows [16,17]:

$$\mathbf{D}_1 = F_{\text{XUV}} \sum_j (\mathbf{d}_{l,q}(\mathbf{K}'_j) \cdot \mathbf{e}_{\text{XUV}}) \mathbf{g}(t_j, t'_j), \quad (10)$$

where  $\mathbf{K}'_j \equiv \mathbf{K}(t'_j; t_j, t'_j)$  is the electron momentum at the ionization time,  $\mathbf{d}_{l,q}$  is the dipole matrix element describing the transition from the bound state  $\psi_{l,q}(\mathbf{r}) = \varphi_l(r) f_{l,q}(\hat{\mathbf{r}})$  to the continuum state  $\psi_{\mathbf{K}'_j}^{(+)}(\mathbf{r})$  having the outgoing spherical wave asymptotics at long distances,

$$\mathbf{d}_{l,q}(\mathbf{k}) = \langle \varphi_{l,q}(\mathbf{r}) | \mathbf{r} | \psi_{\mathbf{k}}^{(+)}(\mathbf{r}) \rangle. \quad (11)$$

The vector  $\mathbf{g}(t_j, t'_j)$  describes the electron propagation and recombination stages and defines the polarization of the emitted harmonics. The explicit form of the specified factor may be found in [16,18].

If the atomic system has an optically active  $s$ -electron, then  $\psi_{l,q}(\mathbf{r}) = \varphi_0(r) Y_{0,0}(\hat{\mathbf{r}})$ , and integration by angular variables in the matrix element (11) results in:

$$\mathbf{d}_{0,0}(\mathbf{k}) = \frac{1}{4\pi} \frac{\mathbf{k}}{k} \mathcal{D}_{0,1}(k), \quad (12)$$

where  $\mathcal{D}_{0,1}(k)$  is the radial matrix element:

$$\mathcal{D}_{l,l'}(k) = \langle R_{k,l'}(r) | r | \varphi_l \rangle, \quad (13)$$

$$\psi_{\mathbf{k}}^{(+)}(\mathbf{r}) = \sum_{l,m} R_{k,l}(r) Y_{l,m}^*(\hat{\mathbf{k}}) Y_{l,m}(\hat{\mathbf{r}}). \quad (14)$$

In terms of the three-step model of the HHG, electron should return to the parent core. For the two-component field with the orthogonal component polarization (1), electron motion in the continuum is defined only by the low-frequency component, and the electron momentum should be parallel to the IR field polarization vector. Thus,  $\mathbf{d}_{0,0}(\mathbf{K}'_j) = d_{0,0}(\mathbf{K}'_j) \mathbf{e}_{\text{IR}}$ , and the scalar product in (10) vanishes. This results in the XUV-induced HHG process being forbidden by the dipole selection rules in the framework of the adiabatic approximation, and HHG in this channel is defined by small corrections to the results obtained within the adiabatic approximation.

If the atomic system has the valence  $p$ -electron, then the coupled state is triply degenerate in the magnetic quantum number. During the interaction with the laser pulse written as (1), the degeneracy is fully removed, and three isolated sublevels are formed for which the angular part of the wave function is written as

$$f_{1,0}(\hat{\mathbf{r}}) = Y_{10}(\hat{\mathbf{r}}), \quad (15a)$$

$$f_{1,\pm 1}(\hat{\mathbf{r}}) = i^{\frac{3\mp 1}{2}} \frac{Y_{1,1}(\hat{\mathbf{r}}) \pm Y_{1,-1}(\hat{\mathbf{r}})}{\sqrt{2}}. \quad (15b)$$

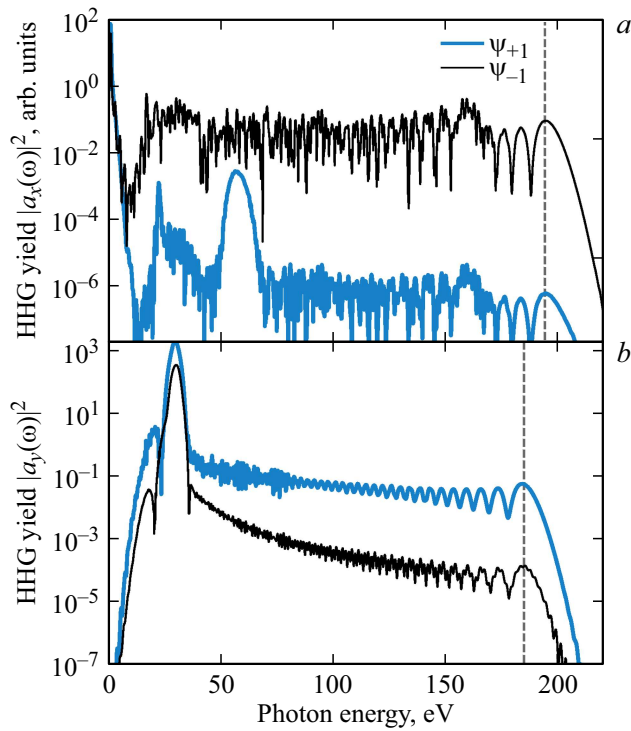


**Figure 2.** The yield of high-order harmonics polarized along the IR field polarization vector (a) and XUV pulse polarization vector (b) vs. photon energy. Thick blue line: the result for the state with  $q = +1$ ; thin black line: the result for the state with  $q = -1$ . Vertical dashed lines denote the plateau cutoff position. The field parameters are the same as for Figure 1.

The main contribution to HHG in the two-component field with orthogonal component polarization is made by sublevels with  $q = \pm 1$ . Performing the integration by angular variables for the given states, we get:

$$\mathbf{d}_{1,+1}(\mathbf{K}'_j) = \sqrt{\frac{3}{4\pi}} \left[ \frac{D_{1,0}(\mathbf{K}'_j) - D_{1,2}(\mathbf{K}'_j)}{3} \mathbf{e}_y + D_{1,2}(\mathbf{K}'_j) \frac{(\mathbf{K}'_j \cdot \mathbf{e}_y)}{K_j'^2} \mathbf{K}'_j \right], \quad (16a)$$

$$\mathbf{d}_{1,-1}(\mathbf{K}'_j) = \sqrt{\frac{3}{4\pi}} \left[ \frac{D_{1,0}(\mathbf{K}'_j) - D_{1,2}(\mathbf{K}'_j)}{3} \mathbf{e}_x + D_{1,2}(\mathbf{K}'_j) \frac{(\mathbf{K}'_j \cdot \mathbf{e}_x)}{K_j'^2} \mathbf{K}'_j \right]. \quad (16b)$$

Assuming that  $\mathbf{K}'_j = K'_j \mathbf{e}_x$ , the dipole matrix element  $\mathbf{d}_{1,+1}/\mathbf{d}_{1,-1}$  is directed along the XUV/IR pulse polarization vector. For the initial state with  $q = -1$ , which makes the main contribution to HHG in the single-component IR field, harmonic generation in the XUV-induced channel is suppressed as in the case of the initial  $s$ -state. However, the state with  $q = +1$  makes the main contribution to the generation of harmonics polarized along  $\mathbf{e}_y$ . HHG

probability in this channel is comparable with HHG probability in the IR-induced channel for the state with  $q = -1$ . Figure 2 shows the partial yields of high-order harmonics polarized along the IR (a) and XUV (b) pulse polarization directions for the states with  $q = \pm 1$ . It is shown that the main contribution to the formation of harmonics with the polarization vector  $\mathbf{e}_h = \mathbf{e}_{\text{IR}}$  occurring as a result of the IR-induced HHG process is made by the state with  $q = -1$ . At the same time, the yield of harmonics with polarization  $\mathbf{e}_h = \mathbf{e}_{\text{XUV}}$  produced by the XUV-induced process is mainly defined by the contribution of the state with  $q = +1$ . It should be noted that harmonics in the XUV-induced and IR-induced channels have close intensities, and this may be used to control the secondary radiation polarization for atomic systems with the valence  $p$ -electron in the two-component laser field with orthogonal geometry [16].

In summary, in this work we have investigated the effect of the initial state symmetry on the HHG process by the atomic system in the two-component pulse whose IR and XUV components are linearly polarized in mutually perpendicular directions. Based on the adiabatic approximation for HHG description, it has been shown that the harmonic generation process with XUV photon absorption at the ionization stage appears to be suppressed for the initial  $s$ -state of the optically active electron. For the triply degenerate initial  $p$ -state, the XUV-induced process appears to be possible for one of three magnetic sublevels, which allows the HHG intensity in the XUV-induced channel to be increased considerably. It should be noted that the effects of harmonic propagation in the medium shall be considered to find the macroscopic HHG spectra by actual atomic systems [19,20]. The description of the macroscopic effects is beyond the scope of this study because they do not result in any change in the role played by the initial state symmetry in the HHG process.

## Funding

This study was supported by the Russian Science Foundation (grant № 22-12-00223).

## Conflict of interest

The authors declare that they have no conflict of interest.

## References

- [1] T. Popmintchev, M.-C. Chen, P. Arpin, M.M. Murnane, H.C. Kapteyn. *Nat. Photon.*, **4** (3), 822 (2010). DOI: 10.1038/nphoton.2010.256
- [2] T. Popmintchev, M.-C. Chen, D. Popmintchev, P. Arpin, S. Brown, S. Ališauskas, G. Andriukaitis, T. Balčiūnas, O.D. Mücke, A. Pugzlys, A. Baltuška, B. Shim, S.E. Schrauth, A. Gaeta, C. Hernández-García, L. Plaja, A. Becker, A. Jaron-Becker, M.M. Murnane, H.C. Kapteyn. *Science*, **336** (6086), 1287 (2012). DOI: 10.1126/science.1218497

- [3] D. Popmintchev, B.R. Galloway, M.-C. Chen, F. Dollar, C.A. Mancuso, A. Hankla, L. Miaja-Avila, G. O’Neil, J.M. Shaw, G. Fan, S. Ališauskas, G. Andriukaitis, T. Balčiunas, O.D. Mücke, A. Pugzlys, A. Baltuška, H.C. Kapteyn, T. Popmintchev, M.M. Murnane. *Phys. Rev. Lett.*, **120** (9), 093002 (2018). DOI: 10.1103/PhysRevLett.120.093002
- [4] P. Agostini, L.F. DiMauro. *Rep. Prog. Phys.*, **67** (6), 813 (2004). DOI: 10.1088/0034-4885/67/6/R01
- [5] P.B. Corkum, F. Krausz. *Nat. Phys.*, **3** (6), 381 (2007). DOI: 10.1038/nphys620
- [6] F. Krausz, M. Ivanov. *Rev. Mod. Phys.*, **81** (1), 163 (2009). DOI: 10.1103/RevModPhys.81.163
- [7] P.B. Corkum. *Phys. Rev. Lett.*, **71** (13), 1994 (1993). DOI: 10.1103/PhysRevLett.71.1994
- [8] G. Gademann, F. Kelkensberg, W.K. Siu, P. Johnsson, M.B. Gaarde, K.J. Schafer, M.J.J. Vrakking. *New J. Phys.*, **13** (3), 033002 (2011). DOI: 10.1088/1367-2630/13/3/033002
- [9] D. Azoury, M. Krüger, G. Orenstein, H.R. Larsson, S. Bauch, B.D. Bruner, N. Dudovich. *Nat. Comm.*, **8** (1), 1453 (2017). DOI: 10.1038/s41467-017-01723-w
- [10] D. Kiewewetter, R.R. Jones, A. Camper, S.B. Schoun, P. Agostini, L.F. DiMauro. *Nature Physics*, **14** (1), 68 (2018). DOI: 10.1038/nphys4279
- [11] M. Krüger, D. Azoury, B.D. Bruner, N. Dudovich. *Appl. Sci.*, **9** (3), 378 (2019). DOI: 10.3390/app9030378
- [12] K.J. Schafer, M.B. Gaarde, A. Heinrich, J. Biegert, U. Keller. *Phys. Rev. Lett.*, **92** (2), 023003 (2004). DOI: 10.1103/PhysRevLett.92.023003
- [13] J. Biegert, A. Heinrich, C.P. Hauri, W. Kornelis, P. Schlup, M.P. Anscombe, M.B. Gaarde, K.J. Schafer, U. Keller. *J. Mod. Opt.*, **53** (1–2), 87 (2006). DOI: 10.1080/09500340500167669
- [14] J. Tate, T. Augustine, H.G. Muller, P. Salières, P. Agostini, L.F. DiMauro. *Phys. Rev. Lett.*, **98** (1), 013901 (2007). DOI: 10.1103/PhysRevLett.98.013901
- [15] M.V. Frolov, N.L. Manakov, W.-H. Xiong, L.-Y. Peng, J. Burgdörfer, A.F. Starace. *Phys. Rev. A*, **92** (2), 023409 (2015). DOI: 10.1103/PhysRevA.92.023409
- [16] T.S. Sarantseva, A.A. Romanov, A.A. Silaev, N.V. Vvedenskii, M.V. Frolov. *Phys. Rev. A*, **107** (2), 023113 (2023). DOI: 10.1103/PhysRevA.107.023113
- [17] A.A. Romanov, A.A. Silaev, M.V. Frolov, N.V. Vvedenskii. *Phys. Rev. A*, **101** (1), 013435 (2020). DOI: 10.1103/PhysRevA.101.013435
- [18] A.V. Flegel, N.L. Manakov, I.V. Breev, M.V. Frolov. *Phys. Rev. A*, **104** (3), 033109 (2021). DOI: 10.1103/PhysRevA.104.033109
- [19] P. Salières, A. L’Huillier, M. Lewenstein. *Phys. Rev. Lett.*, **74** (19), 3776 (1995). DOI: 10.1103/PhysRevLett.74.3776
- [20] M.B. Gaarde, J.L. Tate, K.J. Schafer. *J. Phys. B: At. Mol. Opt. Phys.*, **41** (13), 132001 (2008). DOI: 10.1088/0953-4075/41/13/132001

*Translated by E.Iinskaya*